Computer-Aided Filter Alignment and Diagnosis

HERBERT L. THAL, JR., MEMBER, IEEE

Abstract—**The cavity resonant frequencies and coupling values of a wide range of bandpass filters, band-reject filters, and equalizers have been determined *in situ* by computer-adjusting analytic models to fit the scattering parameters measured on an automatic network analyzer. A higher order mode elliptic filter, a dual-mode quasi-elliptic filter, and a dual-mode band-reject filter are presented as examples. The general relationships between mechanical dimensions and circuit parameters are discussed. The circuit adjustment procedure is outlined, and equations for the sensitivity coefficients of several element types are tabulated.**

I. Description of Method

EQUIVALENT-circuit analysis programs with element optimization routines have been incorporated into the software library of an automatic network analyzer (ANA) (Hewlett–Packard 8542). After ANA measurements of a filter are taken, the element values of the appropriate circuit are computer-adjusted in the manner outlined in Section V to provide a best fit representation of the experimental filter. Since each element in a suitably constructed equivalent circuit may be related to some physical portion of the actual filter, the changes required to converge to the nominal response are evident. In addition to providing a convenient method for diagnosing and correcting coupling and tuning errors in filters, this procedure provides an indication of the accuracy of the experimental data and the adequacy of the analytic models, thereby increasing confidence in system designs and simulations which are based on these same models.

The alignment of a filter by this method involves the following steps:

1) measure the complex scattering parameters of the filter;
2) transfer the experimental data to disk;
3) load the desired circuit program and recall the data;
4) select the frequency range and scattering parameters to be used in the fitting; note that S_{12} cannot be used alone since by reciprocity it remains unchanged if the filter is reversed and hence cannot resolve one end from the other;
5) enter an initial estimate of the synchronous frequency, coupling values, and Qu (e.g., the nominal design values);
6) use the cavity frequencies and coupling values from the best fit circuit to determine the required filter adjustments;
7) recall the measurement program and iterate.

Manuscript received May 24, 1978; revised July 28, 1978.
The author is with the Valley Forge Space Center, General Electric Company, Box 8555, Philadelphia, PA 19101.

This method has been used on Chebyshev and elliptic filters with up to 13 poles in single- , dual- , and higher order mode realizations. It has been used for aligning the frequencies and nulling the spurious cross-coupling in directionally coupled equalizer stages as well. Both discrete element and inductively loaded waveguide circuit models have been used; other configurations could be implemented. In addition, filter circuits have been synthesized by replacing the experimental scattering parameters with ones generated from a desired pole-zero pattern.

II. TE_{011} Filter

A six-pole TE_{011} elliptic filter is used to illustrate this technique. Its stacked (folded-back) cavity arrangement is similar to that described by Atia and Williams [1]. An appropriate distortion of the basic cylindrical cavity shape separates the frequency of the degenerate TM_{111} (doublet) modes by more than 5 percent while at the same time providing a slight increase in the unloaded Q. Fig. 1 shows the experimental transmission and reflection losses, i.e., the reciprocals of $|S_{12}|$ and $|S_{11}|$ in decibels, with relatively severe detuning of some cavities. Each curve is computer drawn from 101 data points taken at 1-MHz intervals. For filters with this narrow a bandwidth, a discrete element circuit is adequate. Each resonator is represented by series *RLC* elements with magnetic coupling between arbitrarily specified resonator pairs. The mutual inductances, cavity capacitances, and output waveguide reference planes are varied to match the measured response; the cavity resonant frequencies are then calculated from the capacitances. Fig. 2 shows the diagnostic printout from this procedure using the complex scattering parameters at 34 of the measured frequencies. The mutual inductive coupling values are expressed in terms of the resonant frequency splitting (megahertz) that would occur for the respective cavity pair if all other cavities were detuned [2]; a negative sign indicates coupling of the opposite sense. Fig. 3 gives analytic responses obtained from these values.

Since each cavity is tuned by moving one of its end walls in or out, the tuning sensitivity (e.g., megahertz/turn) is essentially linear and readily calculated (or measured). Thus each plunger may be turned the amount required to tune it from the frequency given in Fig. 2 to the desired synchronous frequency. Fig. 4 shows the responses after retuning, and Fig. 5 gives the new circuit parameters from the fitting procedure. Note that the repeatability of the coupling values of the unmodified apertures is good even though the filter was removed and the

0018-9480/78/1200-0958$00.75

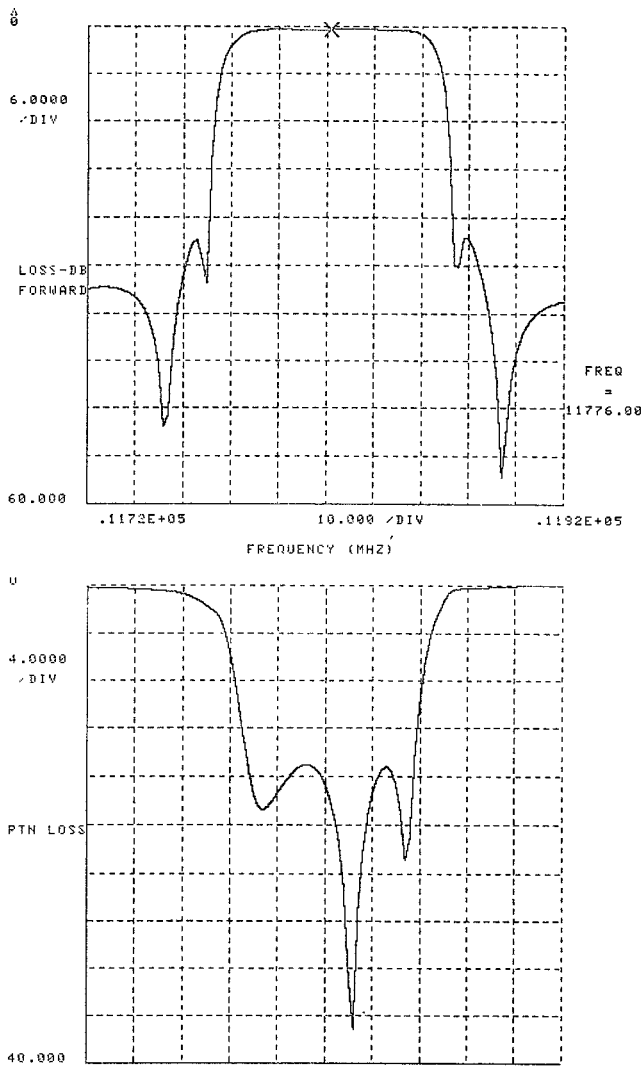

Fig. 1. Experimental insertion and return loss for misaligned filter.

			COUPLING	FREQ(MHZ)
1	0	1	42.0094	11775.2
2	1	2	35.5747	11779.2
3	2	3	21.5797	11781.5
4	3	4	36.9634	11769.9
5	4	5	22.0643	11772.9
6	5	6	36.3145	11770.7
7	6	7	41.4987	
8	2	5	-17.4086	
9	1	6	4.6906	
Q1,Q2			200.3	200.8
REF PLANES(CM)			.226	.224

Fig. 2. Coupling values and frequencies from fitting procedure using data of Fig. 1.

analyzer was recalibrated between the two runs. Fig. 6 shows the reconstructed responses. The unloaded Q is determined semiautomatically by repeating the fitting procedure with different values and selecting the one that yields the best fit; the unloaded Q for this filter is 20 000.

The coupling between cavities is proportional to the magnetic polarizability [2], [3] of the aperture (and also to the square of the magnetic field at the aperture per unit energy stored in the cavity). The dominant polarizability

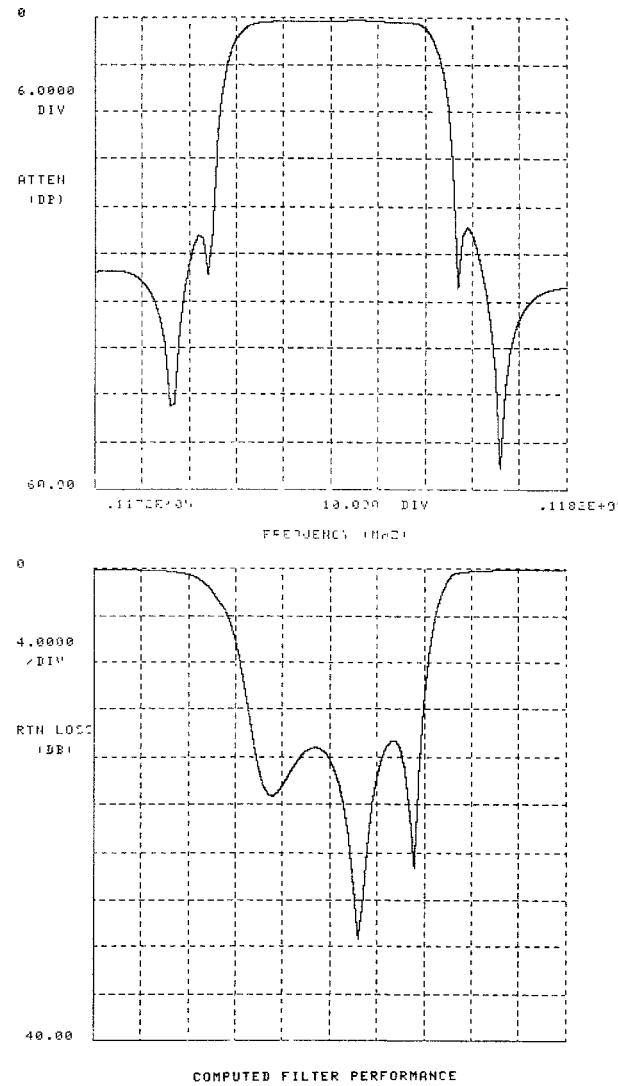

Fig. 3. Computed response using values from Fig. 2.

component generally is proportional to the cube of the aperture dimensions (with corrections for thickness and resonance). The apertures can be modified in this manner to converge to the desired coupling even when unusual aperture and cavity shapes are involved; the results obtained with each new configuration increase the data base for making further predictions or estimating variations in coupling due to mechanical tolerances.

III. Dual-Mode Filter

A second example is provided by an eight-pole dual-mode [4], [5] quasi-elliptic filter. Fig. 7 shows the internal construction of a similar filter. Each cavity has a pair of tuning screws for the orthogonal TE_{111} resonances plus a coupling screw at a 45° orientation. Both resonant modes are coupled to the correspondingly polarized modes in the adjacent cavity by an end-wall aperture. (The thin slot in the figure yields a large difference between the coupling values for the parallel and perpendicular polarized cases.) Fig. 8 gives a diagnostic output based on fitting S_{11}, S_{12}, and S_{22} at 41 frequencies with a 3-MHz spacing. The rms value indicates the rms deviation of a reconstructed (com-

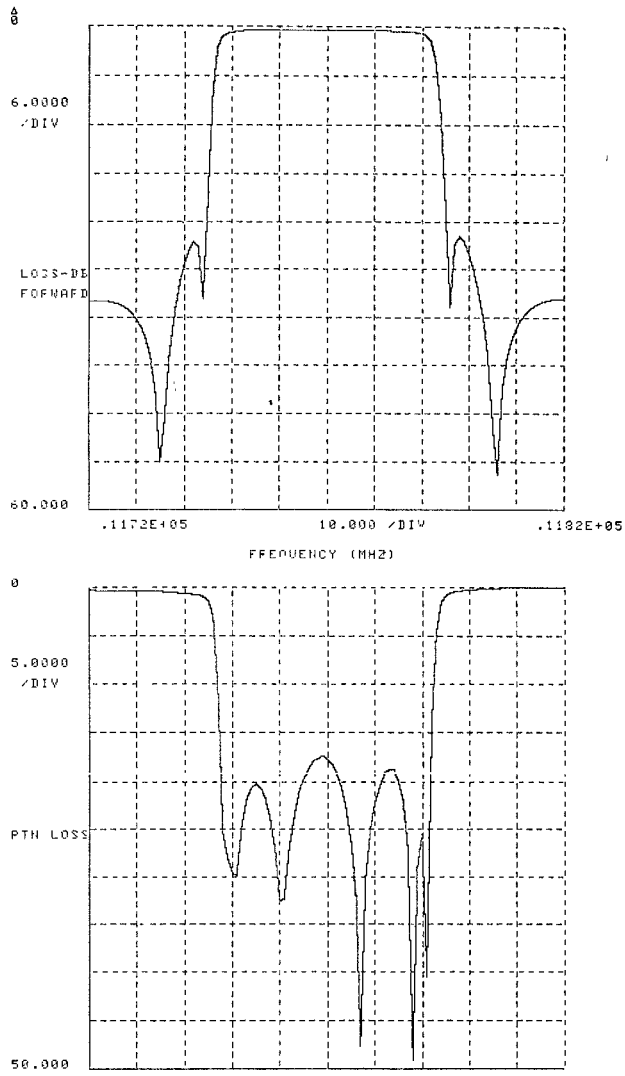

Fig. 4. Experimental insertion and return loss for aligned filter.

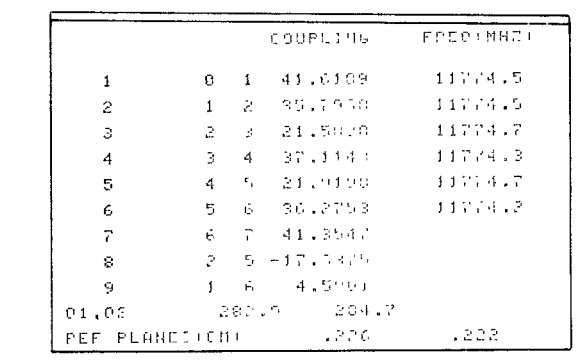

			COUPLING	FREQ(MHZ)
1	0	1	41.6109	11774.5
2	1	2	35.7938	11774.5
3	2	3	31.5020	11774.7
4	3	4	30.1141	11774.3
5	4	5	31.0120	11774.7
6	5	6	30.2758	11774.3
7	6	7	41.3547	
8	2	5	-17.7475	
9	1	6	4.5700	
01.02		280.5	284.7	
REF PLANE(CM)			.220	.222

Fig. 5. Coupling values and frequencies from fitting procedure using data of Fig. 4.

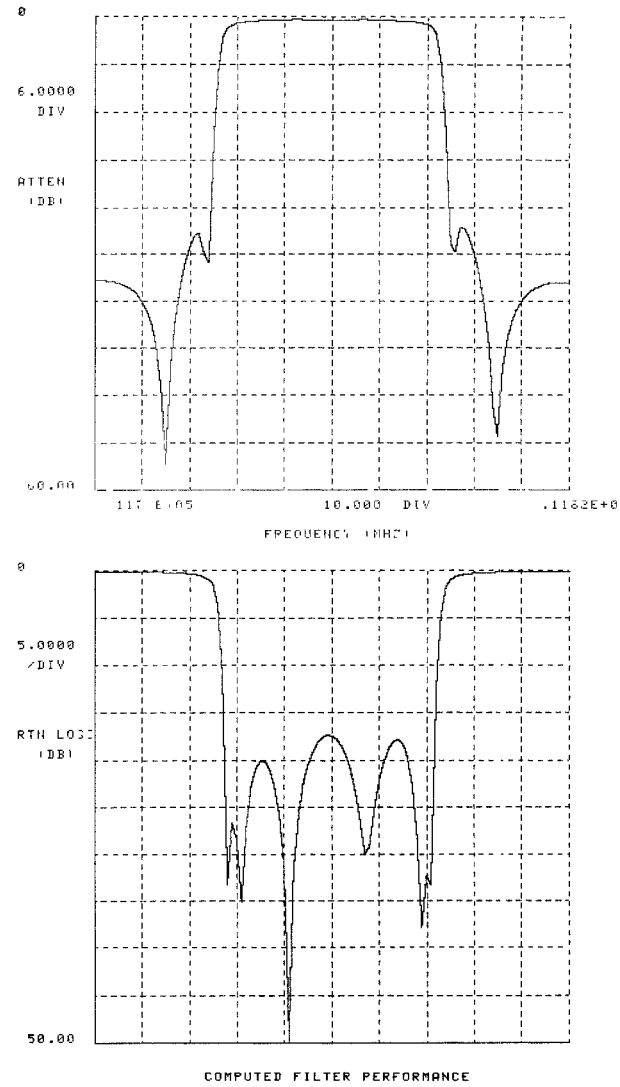

Fig. 6. Computed response using values from Fig. 5.

plex) S-parameter value from the experimental. The three parameters varied by the screws in each of the four cavities have been enclosed in boxes. The two coupling values controlled by each of the three internal apertures have been connected by arrows.

Although each of the three screws (per cavity) performs a different nominal function, there are some interactions which are nonlinear with depth. For example, increasing the penetration of a tuning screw causes a (capacitive) decrease in the frequency of the mode having its electric field parallel to the screw axis and a lesser (inductive) increase in the orthogonal mode. The following empirical equations (which are consistent with theoretical expectations) relate the tuning to the screw penetration turns N.

$$\Delta f_c = -[2AN + BN^3] \quad \text{(capacitive)} \tag{1}$$

$$\Delta f_L = +AN \quad \text{(inductive).} \tag{2}$$

The values of A and B may be determined by measuring the two frequency shifts near the maximum anticipated N; this filter has A and $B=2.25$ and 0.275 MHz for 0.072-in diameter tuners with a 0.0125-in penetration per turn. The two modes of the coupled system have their electric fields parallel and perpendicular to the 45° coupling screw. Their frequency separation corresponds to the coupling in Fig. 8 and is given by

$$\Delta f_x = 3AN_x + BN_x^3 \quad \text{(coupling)} \tag{3}$$

where N_x is the coupling screw penetration.

The tuning of mode 1 is determined primarily by its own capacitive tuning screw modified by the inductive effect of the orthogonal tuning screw and one-half the net

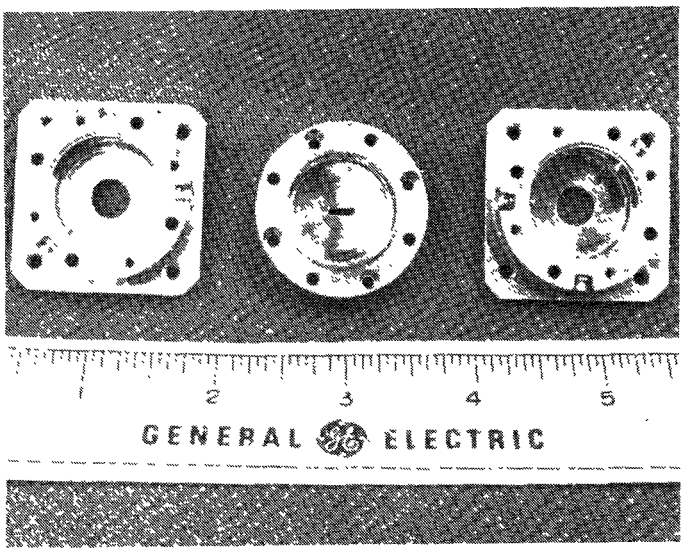

Fig. 7. Internal view of dual-mode filter.

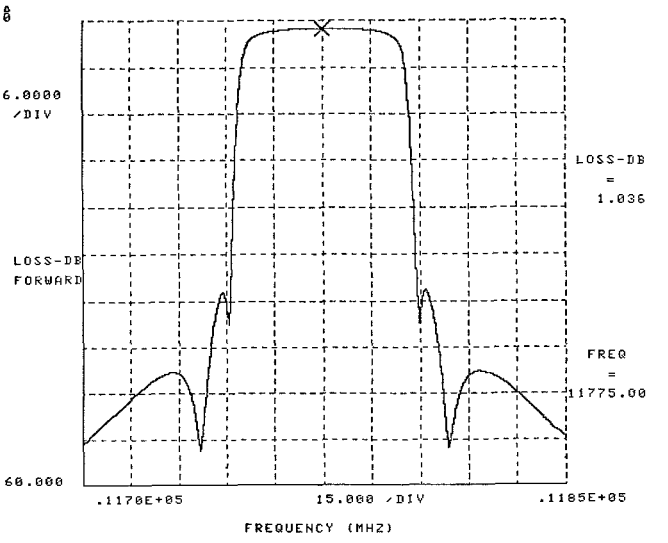

Fig. 9. Insertion loss of dual-mode filter after further alignment based on the diagnostic information of Fig. 8.

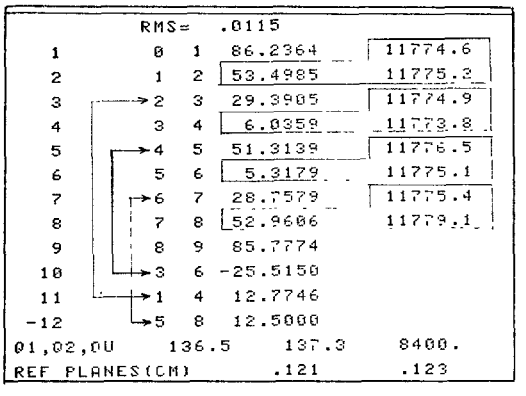

			RMS= .0115	
1	0	1	86.2364	11774.6
2	1	2	53.4985	11775.3
3	2	3	29.3905	11774.9
4	3	4	6.0359	11773.8
5	4	5	51.3139	11776.5
6	5	6	5.3179	11775.1
7	6	7	28.7579	11775.4
8	7	8	52.9606	11779.1
9	8	9	85.7774	
10	3	6	-25.5150	
11	1	4	12.7746	
-12	5	8	12.5000	
01,02,0U	136.5		137.3	8400.
REF PLANES(CM)			.121	.123

Fig. 8. Preliminary coupling values and frequencies for an eight-pole dual-mode filter. The three parameters in each box are controlled by the three screws in each of the four cavities. The pairs of coupling values connected by arrows correspond to the orthogonal polarizations coupled through each of the three internal apertures.

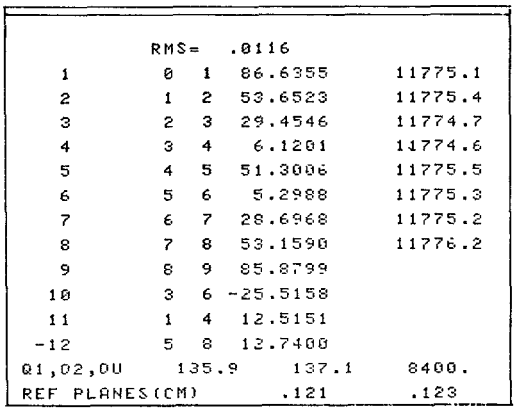

			RMS= .0116	
1	0	1	86.6355	11775.1
2	1	2	53.6523	11775.4
3	2	3	29.4546	11774.7
4	3	4	6.1201	11774.6
5	4	5	51.3006	11775.5
6	5	6	5.2988	11775.3
7	6	7	28.6968	11775.2
8	7	8	53.1590	11776.2
9	8	9	85.8799	
10	3	6	-25.5158	
11	1	4	12.5151	
-12	5	8	12.7400	
01,02,0U	135.9		137.1	8400.
REF PLANES(CM)			.121	.123

Fig. 10. Coupling values and frequencies corresponding to the response of Fig. 9.

capacitive/inductive effect of the coupling screw; that is

$$\Delta f_1 = -A\left[2N_1 - N_2 + \tfrac{1}{2}N_x\right] - B\left[N_1^3 + \tfrac{1}{2}N_x^3\right] \quad \text{(tuning)}. \tag{4}$$

The same equation applies to mode 2 if subscripts 1 and 2 are interchanged. An auxiliary computer program is used to predict new screw depths based on the coupling and resonant frequencies indicated by the diagnostic output, the desired values, and the present depths. (It is estimated that in order to take full advantage of this procedure it will be necessary to increase the mechanical accuracy to which the screws can be set.) The gross tuning of all three screws reduces the unloaded Q of the cavity [6].

Fig. 9 shows the experimental response of the filter after further adjustment; the corresponding coupling values and resonant frequencies are shown in Fig. 10. For this filter, the sensitivities of the S parameters to coupling values 1–4 and 5–8 are so nearly equal across the frequency band that unique values for both cannot be determined. This is resolved by holding 5–8 fixed as indicated by the minus sign in front of the 12. Since the filter is nominally symmetric, the average value may be assumed for each; either coupling slot (or both) may be modified to achieve small corrections to the coupling if necessary so that the inability to determine the exact contribution of each is not a practical concern.

Changes in the end-wall coupling apertures may be made in the manner described for the TE_{011} filter except that for the dual-mode filter each aperture provides two coupling values (although in some cases one of them may be very small). The simplest approach is to use a pair of thin crossed slots since each length (cubed) will provide essentially independent adjustment of one coupling. However, this technique may result in an undesired reduction in the unloaded Q [6] particularly for broad-band filters. An "elliptical" aperture [2] yields a lower loss but introduces an interdependence between both dimensions and both couplings.

IV. Band-Reject Filter

A dual-mode band-reject filter may be formed by coupling a cylindrical cavity asymmetrically to the broad wall of a rectangular waveguide to equally excite both TE_{111} modes and then providing cross-coupling between these

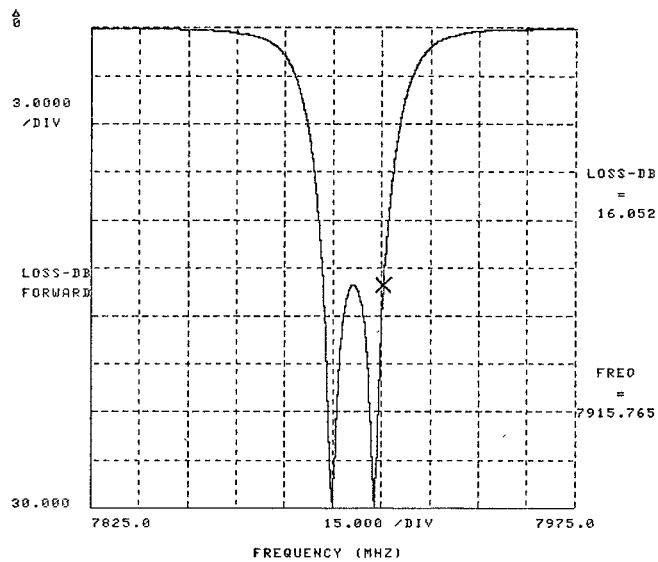

Fig. 11. Insertion loss of two-pole band-reject filter.

	RMS=	.0080		
1	0	1	21.4195	7906.3
2	1	2	24.9466	7906.4
3	2	3	20.9901	
Q1,Q2,QU	369.1		376.6	9200.
REF PLANES(CM)			.018	-.010

Fig. 12. Coupling values and frequencies corresponding to the response of Fig. 11.

modes by some means such as a 45° screw. The same diagnostic program used for the preceding filters may be applied to this case by first transforming the experimental data into equivalent odd- and even- mode excitations (i.e., push–push and push–pull) in the rectangular waveguide using the relations

$$S_{OO} = -S_{12} + \tfrac{1}{2}[S_{11} + S_{22}] \tag{5}$$

$$S_{EE} = -S_{12} - \tfrac{1}{2}[S_{11} + S_{22}] \tag{6}$$

$$S_{OE} = j\tfrac{1}{2}[S_{11} - S_{22}]. \tag{7}$$

Fig. 11 shows the transmission loss of a two-pole (single-cavity) filter of this type. The diagnostic results are given in Fig. 12. The 0–1 coupling and the $Q1$ value correspond to the excitation of the odd-TE_{111} resonance, and the 2–3 coupling to the even. Moving the cylindrical cavity towards the side wall of the rectangular guide increases the even-mode coupling and decreases the odd. Additional cavities can be stacked to increase the order of the response (two poles per cavity).

V. Circuit Adjustment Procedure

Fig. 13 illustrates a schematic diagram of a filter circuit including the matched terminating impedances of the input and output lines, a single representative internal impedance element, and a source at the port-1 end. The superscript 1 on the currents and voltages indicates that

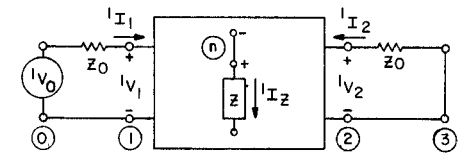

Fig. 13. Schematic diagram of a filter showing a representative circuit element.

they are due to this source. Assume that a voltage generator V_n is inserted at port n which is normally short-circuited. Then the change in the value of $^1I_1$ is given by

$$\Delta^1 I_1 = V_n \left[\frac{^1I_z}{^1V_0} \right] \tag{8}$$

since the transfer admittance between ports 0 and n is reciprocal. This generator can be used to simulate changes in the value of the impedance Z by letting

$$V_n = -(^1I_z + \Delta^1 I_z)\Delta Z \approx -^1I_z \Delta Z \tag{9}$$

for small changes. The reflection coefficient S_{11} is given by

$$S_{11} = \frac{^1V_1 - ^1I_1 Z_0}{^1V_1 + ^1I_1 Z_0} = 1 - 2\frac{^1I_1 Z_0}{^1V_0} \tag{10}$$

so that changes in S_{11} and $^1I_1$ are related by

$$\Delta S_{11} = -2\frac{\Delta^1 I_1 Z_0}{^1V_0}. \tag{11}$$

An approximate relationship between ΔS_{11} and ΔZ for small perturbations is obtained from (8), (9), and (11).

$$\Delta S_{11} \approx 2\left[\frac{^1I_z Z_0}{^1V_0} \right]^2 \left[\frac{\Delta Z}{Z_0} \right]. \tag{12}$$

The sensitivity of S_{12} may be found in a similar manner, but it is necessary to analyze the circuit a second time with a source at the port-2 end in order to establish the relationship between V_n and ΔI_2. Once the sensitivity coefficients have been found, an equation of the following form can be written for each frequency and S parameter.

$$\varepsilon = -^eS + S + A_1\delta_1 + A_2\delta_2 + \cdots + A_k\delta_k + \cdots + A_N\delta_N \tag{13}$$

where

- ^eS (complex) experimental value of S_{11}, S_{12}, or S_{22},
- S prediction of the present circuit,
- A_k (complex) sensitivity coefficient of the kth element,
- δ_k (real) change in element value,
- ε residual error between the experimental and computed values after adjustment of the circuit.

The number of (complex) equations (e.g., 3×41 for the dual-mode quasi-elliptic example) in general, greatly exceeds the number of variable elements (21 for the same example); these equations are solved for a least sum squared value of $\|\epsilon\|$. Since (13) represents a linearization

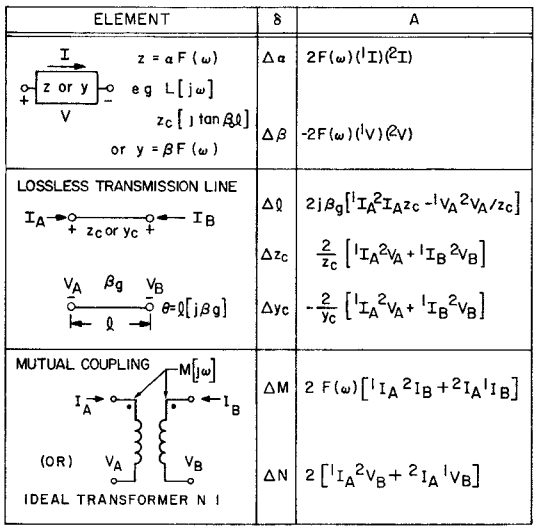

Fig. 14. Tabulation of expressions for sensitivity coefficients for circuit elements used in filter equivalent circuits. All values normalized to $Z_0 = 1\ \Omega$ and ${}^1V_0$ or ${}^2V_0 = 1$ V.

of the effects of the element changes, it generally is necessary to iterate the procedure a few times. Fig. 14 provides a tabulation of S_{12} sensitivity coefficients for various element types. All currents, voltages, and impedances are assumed to be normalized to the case where $Z_0 = 1\ \Omega$ and ${}^1V_0$ or ${}^2V_0 = 1$ V. The values for S_{11} or S_{22} may be obtained as special cases by letting all superscripts be 1 or 2, respectively.

Acknowledgment

The author wishes to acknowledge the contributions of G. Ditty to the design and testing of the experimental models, and L. Bickel to the ANA software modifications.

References

[1] A. E. Atia and A. E. Williams, "General TE_{011} mode waveguide bandpass filters," *IEEE Trans. Microwave Theory Tech.*, vol. MTT-24, pp. 640–648, Oct. 1976.

[2] G. L. Matthaei, L. Young, and E. M. T. Jones, *Microwave Filters, Impedance-Matching Networks, and Coupling Structures*. New York: McGraw-Hill, 1964, pp. 231–235, pp. 511–513.

[3] S. B. Cohn, "Determination of aperture parameters by electrolytic tank measurements," *Proc. IRE*, vol. 39, pp. 1416–1421, Nov. 1951.

[4] A. E. Williams, "A four-cavity elliptic waveguide filter," *IEEE Trans. Microwave Theory Tech.*, vol. MTT-18, pp. 1109–1114, Dec. 1970.

[5] R. D. Wanselow, "Prototype characteristics for a class of dual-mode filters," *IEEE Trans. Microwave Theory Tech.*, vol. MTT-23, pp. 708–711, Aug. 1975.

[6] H. L. Thal, "Loss mechanisms in coupled cavity microwave filters," in *IEEE Int. Microwave Symp. Digest*, June 1977, pp. 415–418.

New Results in Network Simulation, Sensitivity, and Tolerance Analysis for Cascaded Structures

JOHN W. BANDLER, FELLOW, IEEE, MOHAMED R. M. RIZK, STUDENT MEMBER, IEEE, AND HANY L. ABDEL-MALEK, STUDENT MEMBER, IEEE

***Abstract*—An attractive, exact, and efficient approach to network analysis for cascaded structures is presented. It is useful for sensitivity and tolerance analyses, in particular, for a multiple of simultaneous large changes in design parameter values. It also facilitates the exploitation of symmetry to reduce computational effort for the analysis. Responses at different loads in branched networks, which may be connected in series or in parallel with the main cascade, can be obtained analytically in terms of the variable elements. Sensitivity and large-change effects with respect to these variables can be easily evaluated. The approach is not confined to 2-port elements but can be generalized to $2p$-port cascaded elements.**

Manuscript received June 15, 1978. This work was supported by the National Research Council of Canada under Grant A7239, and by a Postdoctoral Fellowship awarded to H. L. Abdel-Malek. This paper was presented at the 1978 IEEE Int. Microwave Symp., Ottawa, Ont., Canada, June 27–29, 1978.

J. W. Bandler and M. R. M. Rizk are with the Group on Simulation, Optimization, and Control and the Department of Electrical Engineering, McMaster University, Hamilton, Ont., Canada L8S 4L7.

H. L. Abdel-Malek was with the Group on Simulation, Optimization, and Control and the Department of Electrical Engineering, McMaster University, Hamilton, Ont., Canada L8S 4L7. He is now with the Department of Engineering Physics and Mathematics, Faculty of Engineering, Cairo University, Giza, Egypt.

I. Introduction

THIS PAPER presents a new and comprehensive treatment of computer-oriented cascaded network analysis. The analysis of cascaded networks plays a very important role in the design and optimization of microwave circuits, so that an attractive approach which facilitates efficient analytical and numerical investigations of response, first- and higher, order sensitivities of response, and simultaneous and arbitrary large-change sensitivity evaluation is highly desirable. As is well known, first-

0018-9480/78/1200-0963$00.75 ©1978 IEEE